Blockade of a chemokine, CCL2, reduces chronic colitis-associated carcinogenesis in mice

doi: 10.1158/0008-5472.CAN-09-1451

Blockade of a chemokine, CCL2, reduces chronic colitis-associated carcinogenesis in mice

Boryana Konstantinova Popivanova,[1,2] Feodora Ivanova Kostadinova,[1,2] Kengo Furuichi,[3] Mohamed M. Shamekh,[1] Toshikazu Kondo,[4] Takashi Wada,[5] Kensuke Egashira,[6] and Naofumi Mukaida[1]

[1]Division of Molecular Bioregulation, Cancer Research Institute, Kanazawa University, 13-1 Takara-machi, Kanazawa 920-0934, Japan, [3]Department of Disease Control and Homeostasis, and [5]Department of Laboratory Medicine, Graduate School of Medical Sciences, Kanazawa University, Kanazawa 920-8641, Japan, [4]Department of Forensic Medicine, Wakayama Medical University, Wakayama 641-8509, Japan, and [5]Department of Cardiovascular Medicine, Graduate School of Medical Sciences, Kyushu University, Fukuoka 812-8582, Japan.

[2]These two authors contributed equally.

This work is supported by the Grant-in-Aids from the Ministry of Education, Culture, Sports, Science and Technology of the Japanese Government (B.K.P. and N.M.).

Correspondence should be addressed to Naofumi Mukaida, MD, PhD, Division of Molecular Bioregulation, Cancer Research Institute, Kanazawa University, 13-1 Takara-machi, Kanazawa 920-0934, Japan. Tel: +81-76-265-2767; Fax: +81-76-234-4520; E-mail: naofumim@kenroku.kanazawa-u.ac.jp.

Running title: CCL2 in chronic colitis-associated carcinogenesis

Key Words: chemokine, macrophage, cyclooxygenase-2.

Abstract

Accumulating evidence indicates the crucial contribution of chronic inflammation to various types of carcinogenesis, including colon carcinoma associated with ulcerative colitis and asbestosis-induced malignant mesothelioma. Ulcerative colitis-associated colon carcinogenesis can be recapitulated in mice by azoxymethane (AOM) administration followed by repetitive dextran sulfate sodium (DSS) ingestion. In the course of this carcinogenesis process, the expression of a macrophage-tropic chemokine, CCL2, was enhanced together with intracolonic massive infiltration of macrophages, which were a major source of cyclooxygenase (COX)-2, a crucial mediator of colon carcinogenesis. Mice deficient in CCL2-specific receptor, CCR2, exhibited less macrophage infiltration and lower tumor numbers with attenuated COX-2 expression. Moreover, CCL2 antagonists decreased intracolonic macrophage infiltration and COX-2 expression, attenuated neovascularization, and eventually reduced the numbers and size of colon tumors, even when given after multiple colon tumors have developed. These observations identify CCL2 as a crucial mediator of the initiation and progression of chronic colitis-associated colon carcinogenesis and suggest that targeting CCL2 may be useful in treating colon cancers, particularly those associated with chronic inflammation.

Introduction

Ulcerative colitis (UC) is a major form of inflammatory bowel disease (IBD), an immune-mediated chronic intestinal condition (1). The major symptom of UC is bloody mucoid diarrhea and its clinical course is characterized by repetitive relapses and remissions. Pathological features of UC include prominent leukocyte infiltration in the colonic mucosa and uncontrolled and prolonged inflammatory reactions (1). These conditions frequently cause epithelial dysplasia and DNA damage with microsatellite instability, and eventually can progress to cancer (2). Indeed, involvement of entire colon for longer than 10 years predisposes UC patients to colon cancer (2), indicating the essential contribution of chronic inflammation to colon carcinogenesis. Thus, to develop measures to prevent cancer development in UC patients it is necessary to gain an understanding of the pathogenesis of UC at molecular and cellular levels. Moreover, evidence is accumulating that chronic inflammatory conditions also can cause cancer in other organs as observed on asbestosis and silicosis (3). Thus, elucidation of colon carcinogenesis in UC will also shed a novel light on chronic inflammation-associated carcinogenesis in general.

Oral administration of dextran sulfate sodium (DSS) to rodents is widely used to recapitulate human UC, because it can induce pathological changes similar to that observed in UC patients (4). Moreover, repeated oral DSS ingestion can cause colon carcinoma (5) and this carcinogenesis process is promoted by a prior administration of azoxymethane (AOM), which causes O^6-methyl-guanine formation (6). Activation of NF-κB pathway contributes to this colon carcinogenesis by preventing colon epithelial cell apoptosis and promoting growth factor production by inflammatory cells (7). The crucial involvement of NF-κB activation in colon carcinogenesis prompted us to investigate the roles of the tumor necrosis factor (TNF)-α/TNF receptor axis, because TNF-α is abundantly expressed in colon of patients with IBD (8), and is one of major target molecules of NF-κB and a major activator of NF-κB (9). We showed that combined treatment with AOM and DSS induced the intracolonic expression

of TNF-α, which in turn regulates the trafficking of macrophages and granulocytes, major sources of cycolooxygenase (COX)-2, thereby resulting in the development and progression of colon cancer (10).

TNF-α lacks direct chemotactic activities for macrophages and granulocytes, but can induce the expression of various chemokines in several cell types present in colon tissues such as epithelial cells, fibroblasts, endothelial cells, and leukocytes (9). Thus, it is likely that enhanced TNF-α expression in colon tissues can induce the expression of chemokines active on macrophages and granulocytes. Indeed, the mucosa of patients with IBD exhibited enhanced mRNA and protein expression of MCP-1/CCL2 (11-13), a C-C chemokine with potent chemotactic and activating activities for monocytes/macrophages (14). We previously consistently observed that combined treatment of AOM and DSS enhanced CCL2 mRNA expression in colon tissues and that blocking the TNF-α/TNF receptor axis reduced colorectal carcinogenesis, intracolonic macrophage infiltration, and CCL2 mRNA expression (10). These observations prompted us to investigate the roles of the interaction between CCL2 and its specific receptor, CCR2, in colon carcinogenesis induced by the combined treatment with AOM and DSS. By using CCR2-deficient mice and CCL2 blocking agents, we here document that CCL2 interactions with CCR2 have vital roles in the initiation and progression of colitis-associated colon carcinogenesis.

Materials and Methods

Reagents and antibodies

AOM and DSS (MW 36,000-50,000) were purchased from Sigma-Aldrich, Inc. (St. Louis, MO) and MP Biomedicals Inc. (Aurora, OH), respectively. A specific CCR2 antagonist, propagermanium, was kindly provided by Sanwa Chemical Co. (Osaka, Japan). Human CCL2 N-terminal deleted form (7ND)-expressing vector was prepared by cloning human CCL2 N-terminal deleted cDNA with an epitope FLAG tag in the carboxyl terminal portion to the pcDNA3 expression vector as described previously (15). Rat monoclonal anti-F4/80 antibody was obtained from Serotec (Oxford, United Kingdom). Goat polyclonal anti-COX-2 and mouse monoclonal anti-cytokeratin 20 antibodies were obtained from Santa Cruz Biotechnology (Santa Cruz, CA) and Abcam (Cambridge, UK), respectively. Rabbit polyclonal anti-β-catenin and mouse monoclonal ANTI-FLAG® M2 antibodies were from Sigma-Aldrich, Inc. Rat monoclonal anti-CD31 antibody was from BD Biosciences Pharmingen (Franklin Lakes, NJ). Rabbit polyclonal anti-CCL2 and anti-CCR2 antibodies were prepared by immunizing rabbits with mouse CCL2 protein and CCR2 peptide as previously described (16).

Animal experiments

Pathogen-free 8- to 12-week old female wild-type BALB/c mice (WT) and CCR2-deficient mice, on a BALB/c genetic background, were housed under specific pathogen-free conditions with free access to food and water during the course of experiments. Mice were injected intraperitoneally with 12 mg/kg body weight of AOM dissolved in physiological saline. Five days later, 2 % DSS was given in the drinking water over five days, followed by 16 days of regular water. This cycle was repeated a total of 3 times. Body weights were measured every week and the animals were sacrificed at the indicated time intervals for macroscopical

inspection, histological analysis, and total RNA extraction. In some experiments, 7ND-expressing or pcDNA3 vector was injected into the femoral muscle of WT mice at day 56. Immediately after the injection, a pair of electrode pads was inserted onto the muscle to encompass the injected site, and electrical pulses were delivered 6 times (100V, 50- ms pulse) with an electrical pulse generator (ECM830; BTX, San Diego, CA). At 11 days after the transfection, immunohistochemical analysis detected 7ND protein in the muscle of WT mice receiving 7ND-expressing vector, but not those receiving pcDNA3 vector (Supplemental Fig. 1). In another series of experiments, WT mice were given propagermanium at a dose of 8 mg/kg body weight, mixed with the food, every day from day 56 to day 60. All animal experiments were performed in compliance with the Guideline for the Care and Use of Laboratory Animals of Kanazawa University.

Bone marrow chimeric mice generation

Cell suspensions from male WT or CCR2-deficient bone marrow were prepared from femurs and tibias, filtered and counted. Female WT or CCR2-deficient mice received a single intravenous injection of 1 x 10^7 bone marrow cells, after being irradiated with 4.25 Gy X-rays followed by 4.25 Gy X-rays (MPR-1520R; Hitachi) 4 hours later. The following groups of chimeric mice were generated: WT to WT, WT to CCR2-deficient, CCR2-deficient to WT, and CCR2-deficient to CCR2-deficient mice. Genomic DNA was extracted from blood and bone marrow chimerism was determined 4 weeks later by PCR for the Y chromosome-linked Sry gene (forward, 5'-TGGGACTGGTGACAATTGTC-3'; reverse, 5'-GAGTACAGGTGTGCAGCTCT-3').

Histopathological and immunohistochemical analyses of mouse colon tissues

Resected mouse colon tissues were fixed in 10 % formalin neutral buffer solution (Wako Chemical, Osaka, Japan) for paraffin embedding or were immediately frozen in Tissue-Tek

O.C.T. compound (Sakura Fine Technical Co., Tokyo, Japan) and stored at -80ºC. Paraffin-embedded sections were cut at 5 μm and stained with hematoxylin and eosin solution. Paraffin-embedded sections were additionally deparaffinized for immunohistochemical detection of β-catenin-, CCR2-, CCL2-, F4/80-, Ly-6G-, COX-2-, cytokeratin 20-, and FLAG-positive cells. Frozen sections were used for immunohistochemical detection of mouse CD31-positive cells. Endogenous peroxidase activity was blocked using 3 % H_2O_2 for 5 minutes, followed by incubation with Non-Specific Staining Blocking reagent (DakoCytomation, Carpinteria, CA) for 10 min. The sections were incubated with the optimal dilutions of anti-CCR2, anti-CCL2, anti-F4/80, anti-CD3, anti-β-catenin, anti-COX-2, anti-CD31, anti-cytokeratin 20, or anti-FLAG antibodies overnight at 4ºC. β-catenin- and CCR2-positive cells were detected with horseradish peroxidase (HRP)-labelled anti-rabbit polymer (EnVision+ System, DakoCytomation), while F4/80-positive cells were detected using Catalyzed Signal Amplification (CSA) System (DakoCytomation). Immune complexes were visualized with Peroxidase Substrate DAB kit (Vector Laboratories, Inc., Burlingame, CA). CCL2-, COX-2-, and CD31-positive cells were detected by the incubation with anti-rabbit, anti-goat or anti-rat biotinylated IgG (DakoCytomation, dilution, 1:200). Detection of cytokeratin 20 and FLAG tag was performed with Vector® M.O.M.™ Immunodetection kit (Vector Laboratories, Inc.), according to the manufacturer's instructions. The resultant immune complexes were visualized by ABC *Elite* kit (Vector Laboratories, Inc.) and Peroxidase Substrate DAB kit (Vector Laboratories, Inc.) according to the manufacturer's instructions. Finally, the slides were counterstained with hematoxylin, dehydrated and coverslipped. Positive cells were enumerated on 5 randomly chosen visual fields at x 400 magnification. The pixel numbers of CD31-positive areas were measured on 5 randomly chosen visual fields at x 200 magnification with the aid of Adobe Photoshop software.

A double-color immunofluorescence analysis

Colon tissues were processed to a double-color immunofluorescence analysis using the combination of anti-CCR2 and anti-COX-2 antibodies. Alexa Fluor® 488 donkey anti-rabbit and Alexa Fluor® 546 donkey anti-goat antibodies were used as secondary antibodies. Immunofluorescence was visualized on a Carl Zeiss Laser Scanning Microscope 510.

RT-PCR analysis

Total RNA was extracted from colon tissues with RNeasy® Mini Kit (Qiagen) and 2.5 μg of RNA was reverse-transcribed using ReverTraAce (Toyobo, Japan) and random primers as described previously (10). Thereafter, 2 μl of resultant cDNA was used for amplification using Taq DNA polymerase (Takara Shuzo, Japan) and 10 μM of specific sets of primers with the pre-determined optimal cycle consisting of 94ºC for 30 sec, 55ºC for 1 min and 72ºC for 1 min (Supplemental Table 1) as described previously. The PCR products were fractionated on 1.5 % agarose gel and visualized by ethidium bromide staining. The band intensities were measured with the aid of NIH Image Analysis software version 1.62, and the ratios to GAPDH were determined. Real-time PCR was performed on Applied Biosystems StepOne™ Real-Time PCR System using the comparative C_T quantitation method. TaqMan® Gene Expression Assays (Applied Biosystems, Foster City, CA), containing specific primers (accession numbers: MCP-1/CCL2 – Mm00441242_m1, KC/CXCL1 – Mm00433859_m1, COX-2 – Mm00478374_m1, GAPDH – Mm99999915_g1) and TaqMan® MGB probe (FAM ™ dye-labeled), TaqMan® Fast Universal PCR Master Mix were used with 10 ng of cDNA to detect and quantify the expression levels of CCL2 and COX-2 in mouse colon tissues. GAPDH was amplified as internal control. C_T values of GAPDH were subtracted from C_T values of the target genes (ΔC_T). ΔC_T values of treated mice were compared to ΔC_T values of untreated animals. Reactions were done at 95°C, 20 sec, then 95°C, 00:01, 60°C, 20 sec – 40 cycles.

DNA sequencing and mutation analysis of β-catenin gene

Genomic DNA was extracted from tumor tissues obtained from WT mice receiving either 7ND-expressing or pcDNA3 vector by using NucleoSpin® Tissue Kit (Macherey-Nagel Inc.) according to the manufacturer's instructions. Exon 3 of the β-catenin gene, containing the consensus sequence for glycogen synthase kinase-3β phosphorylation, was amplified by PCR, using specific primers (forward, 5'-GCTGACCTGATGGAGTTGGA-3'; reverse, 5'-GCTACTTGCTCTTGCGTGAA-3') and the following thermal cycling parameters: 35 cycles of 94°C, 5 minutes; followed by 94°C, 45 seconds, 55°C, 1 minute, 72°C, 1 minute; followed by 72°C, 5 minutes. PCR products were subcloned into pSTBlue-1 vector (AccepTor™ vector, Novagen) and sequenced using BigDye® Terminator Ver. 3.1 Cycle Sequencing kit (Applied Biosystems) on an ABI PRISM®3100-*Avant* Genetic Analyzer (Applied Biosystems).

Statistical analysis

The mean±S.D. were calculated for all parameters determined. Statistical significance was evaluated using one-way analysis of variance (ANOVA), and *p* values lower than 0.05 were considered statistically significant.

Results

Enhanced CCL2 expression in the colon during the course of colon carcinogenesis

Consistent with our previous observations (10), a single intraperitoneal injection of the carcinogen AOM, followed by 3 rounds of 2% DSS intake, induced the development of multiple tumors from the middle to distal colon of wild-type (WT) mice (Fig. 1A and Supplemental Fig. 2). Because we previously observed a massive macrophage infiltration during the whole course of this colon carcinogenesis process, we investigated the expression of a macrophage-tropic chemokine MCP-1/CCL2 and its single specific receptor, CCR2. CCL2 mRNA expression level was negligible in untreated WT mice and immediately after AOM treatment, but subsequent to DSS administration CCL2 mRNA expression was augmented (Fig. 1B). CCL2 protein was detected in mononuclear cells infiltrating the lamina propria and submucosal regions, and also in endothelial cells at the earlier phase and colon carcinoma cells at the later phase (Fig. 1C). Immunohistochemical analysis demonstrated that CCR2 was expressed by mononuclear cells infiltrating in the lamina propria and submucosal regions of the colon, and by some colon carcinoma cells during the course of colon carcinogenesis (Fig. 1D).

Reduction in AOM/DSS-induced inflammatory reaction and subsequent tumor formation in the absence of CCR2

A massive infiltration of CCR2-positive cells prompted us to investigate the roles of the CCL2-CCR2 interactions in this colon carcinogenesis. There were no apparent differences in macroscopical and microscopical appearance of the colon of untreated WT and CCR2-deficient mice (Fig. 2A). When both strains were treated with AOM and DSS, WT mice exhibited marked body weight loss and bloody diarrhea, whereas CCR2-deficient mice showed a minimal body weight loss and diarrhea (data not shown). In WT mice, multiple

tumors extended from most of the middle to distal colon by day 56, whereas the numbers and sizes of tumors were remarkably reduced in the colons of CCR2-deficient mice even at day 56 (Fig. 1A and Supplemental Fig. 2). Microscopical analysis consistently demonstrated that WT mice developed severe inflammation with massive infiltration of leukocytes into the mucosa, submucosal edema, and loss of entire crypts and surface epithelium, particularly in the middle to distal colon at day 7 (Fig. 2A). At day 14, inflammatory cell infiltration persisted, accompanied with dysplastic glands with hyperchromatic nuclei, decreased mucin production and dystrophic goblet cells. Moreover, immunohistochemical analysis demonstrated that inflammatory cells consisted of F4/80-positive macrophages (Fig. 2C). At days 28 to 35, adenocarcinomatous lesions with nuclear β-catenin accumulation appeared in the presence of macrophage and granulocyte infiltration, and their sizes and numbers increased progressively, thereafter (Fig. 2A, B). On the contrary, CCR2-deficient mice displayed only mild inflammatory changes in the colon during the course of DSS administration as evidenced by attenuated infiltration of macrophages (Fig. 2C) and eventually developed only a small number of adenocarcinomatous lesions with less nuclear β-catenin accumulation (Fig. 2A, B). These observations identified the CCL2-CCR2 interactions as crucial for the development of chronic inflammation-associated colon carcinoma.

Contribution of CCR2-expressing bone marrow-derived cells to colon carcinogenesis

CCR2 is expressed by non-bone marrow as well as bone marrow-derived cells (17, 18) and we observed CCR2 expression on some cancer cells. Hence, we compared the contribution of CCR2-expressing non-bone marrow- and bone marrow-derived cells to this colon carcinogenesis by using bone marrow chimeric mice prepared from WT and CCR2-deficient mice. Upon combined treatment with AOM and DSS, CCR2-deficient and WT mice transplanted with WT mouse-derived bone marrow cells, developed tumors with a similar

incidence, but at a much higher level than either WT or CCR2-deficient mice transplanted with CCR2-deficient mouse-derived bone marrow (Fig. 3). These observations would indicate that CCR2-expressing bone marrow-derived cells, but not non-bone marrow-derived cells were mainly responsible for tumor development in this model.

Reduction in AOM/DSS-induced expression of COX-2 in CCR2-deficient mice

COX-2 mRNA expression and COX-2-expressing cell number were increased in WT mice following 7 days after the initiation of DSS treatment (Fig. 4A, B, C) as we previously observed (10). In line with our previous observation that COX-2 was expressed by F4/80-positive macrophages, double color immunofluorescence analysis revealed that the cells which expressed CCR2, also expressed COX-2 (Fig. 4D). AOM/DSS-induced increases in COX-2 mRNA expression and COX-2-positive cell numbers, were decreased in the absence of CCR2 (Fig. 4A, B, C). Collectively, AOM/DSS failed to increase the expression of COX-2, an enzyme that is crucially involved in colon carcinoma development, in CCR2-deficient mice.

Reduction of tumor formation by CCR2 antagonist administration

In order to further delineate the role of the CCL2-CCR2 interactions in the progression phase of this colon carcinogenesis model, we administered two distinct types of CCR2 antagonists, 7ND-expressing vector and propagermanium, after three cycles of DSS intake, when multiple colon tumors have developed. When mice were treated with 7ND-expressing vector, the numbers and sizes of macroscopical tumors were markedly reduced (Fig. 5A, B). Histopathological analysis demonstrated that treatment with 7ND-expressing vector attenuated adenocarcinomatous changes (Figure 5C). Likewise, propagermanium treatment reduced the numbers and sizes of tumors and attenuated adenocarcinomatous changes (Supplemental Fig. 3A, B, C). Concomitantly, treatment with 7ND-expressing vector (Fig.

5D) or propagermanium (Supplemental Fig. 3D) decreased the numbers of infiltrating macrophages. 7ND administration reduced intracolonic COX-2 mRNA expression and COX-2-expressing cell numbers (Fig. 6A and Supplemental Fig. 4A). Moreover, 7ND treatment decreased intratumoral CD31-positive vascular areas significantly (Fig. 6B and Supplemental Figure 4B). Similarly, reductions in COX-2 expression and intratumoral vascular areas were observed with propagermanium treatment (Supplemental Fig. 5 and 6). Furthermore, 7ND treatment decreased nuclear accumulation of β-catenin in the tumor cells (Fig. 6C and Supplemental Fig.4C) and the numbers of cytokeratin 20-positive cells (Fig. 6D and Supplmental Fig. 4C). Likewise, propagermanium treatment decreased both β-catenin nuclear accumulation in the tumor cells and cytokeratin 20-positive cell numbers (Supplemental Fig. 7). Finally, the incidence of β-catenin mutations was significantly reduced by 7ND treatment (Supplemental Table 2). Collectively, these observations would indicate that CCL2-CCR2 interactions were also crucially involved in the tumor progression phase after multiple tumors developed, by regulating COX-2-expressing macrophage infiltration.

Discussion

CCL2 was originally identified as a chemokine, which is chemotactic for monocytes and macrophages (14). Although most chemokines can bind several distinct receptors with similar affinities, CCL2 utilizes CCR2 as its single specific receptor (19). Subsequent studies have unraveled the crucial roles of the CCL2-CCR2 interactions in various chronic inflammatory conditions characterized by a macrophage infiltration, such as crescentic glomerulonephritis (20), pulmonary hypertension (21), pulmonary fibrosis (22), atherosclerosis (23), multiple sclerosis (24), and rheumatoid arthritis (25). Moreover, CCL2 mRNA and protein expression was augmented in the mucosa of patients with IBD (11-13). In a recent study, administration of the antioxidant N-acetyl-L-cysteine (NAC) to UC patients had beneficial effects together with down-regulation of CCL2 expression levels (26). We consistently observed that CCL2 protein was detected in mononuclear cells infiltrating the lamina propria and submucosal areas and produced by endothelial cells at early time points. Moreover, genetic deletion of CCR2 protected mice from DSS-induced acute inflammatory changes as previously reported (27). Thus, CCL2-CCR2 interactions can initiate colon carcinogenesis by inducing inflammation in the colon.

In addition to hematopoietic cells such as macrophages, CCR2 is expressed also by non-hematopoietic cells such as endothelial cells (28), fibroblasts (29), and mesenchymal stem cells (30). In line with the previous observation that CCR2 is expressed by prostate cancer cells (31), we detected CCR2 expression on some cancer cells as well as by infiltrating mononuclear cells in this model. However, the analysis of bone marrow chimeric mice revealed that bone marrow-derived CCR2-expressing but not non-bone marrow-derived cells, are indispensable for this colon carcinogenesis, although contribution of bone marrow-derived endothelial progenitor cells (32) and/or fibrocytes (33), cannot be completely excluded.

Andreas and colleagues claimed that upon DSS treatment, CCR2- or CCR5-deficient mice exhibited reduced acute colitis, but with similar level of macrophage infiltration as WT mice (27). On the contrary, combined blockade of CCR2, CCR5, and CXCR3 protected mice from DSS-induced colitis along with a reduction in intracolonic infiltration of CD11b-positive macrophages (34). We also observed that macrophage infiltration was markedly reduced in CCR2-deficient mice after DSS treatment, compared with WT mice. Moreover, intracolonic macrophage infiltration was also reduced by two distinct CCL2 antagonists, 7ND-expressing vector and propagermanium. Thus, CCL2-CCR2 interactions regulate intracolonic infiltration of macrophages under our present conditions.

Solid tumors including colon cancers are infiltrated with leukocytes, which sometimes account for up to 50% of tumor mass, the most represented populations being lymphocytes and macrophages (35). The presence of lymphocytes is considered as evidence of an immunological anti-tumor response, whereas the presence of tumor-associated macrophages (TAM) represents a hallmark of cancer-associated inflammation (35). TAM originate from circulating monocytes which are attracted by chemotactic factors produced locally by tumor cells and resident cells. TAM produce IL-10 and TGF-β to dampen immune response to tumor cells and concomitantly promote tumor growth by producing angiogenic and growth factors. CCL2 was originally identified as a tumor-derived chemotactic factor for macrophages (36). Accumulating evidence indicates that the levels of tumor-derived CCL2 significantly correlate with TAM density and the depth of invasion in cancers of various organs (35). Moreover, experimental studies using xenotransplanted or isotransplanted tumors revealed the involvement of the CCL2-CCR2 axis in cancer invasion and metastasis (37, 16).

In order to clarify the roles of the CCL2-CCR2 in the progression phase of this colon carcinogenesis model, we utilized two different measures to block CCL2 activity; intramuscular injection of 7ND expression vector and administration of propagermanium.

The biological activity of CCL2 depends on the integrity of its N-terminus and 7ND, a mutant protein lacking N-terminal amino acids 2-8, that can form a heterodimer with wild-type CCL2 protein (15), to suppress CCL2 activity (38). Intramuscular transduction of 7ND-expressing vector can result in continuous intramuscular 7ND protein expression and its subsequent secretion into the circulation (39), thereby preventing CCL2-mediated tissue injuries such as vascular remodeling (39), atherosclerosis (39), and renal fibrosis after reperfusion injury (40). Another CCR2 inhibitor, propagermanium, targets glycosylphosphatidylinositol-anchored proteins associated closely with CCR2, and selectively inhibits MCP-1/CCR2 signaling (41). Both measures attenuated intracolonic macrophage infiltration and neovascularization, and eventually reduced the numbers and sizes of colon carcinomas. Thus, it is reasonable to speculate that the CCL2 axis is crucially involved in the progression phase of colon carcinogenesis by regulating macrophage infiltration.

TAM can produce various factors to promote tumor growth and angiogenesis. Among them, prostaglandin E_2 (PGE_2) is presumed to be crucially involved in colon carcinogenesis because it can induce neovascularization (42) and activate a pathway crucial for colon carcinogenesis, the Wnt/β-catenin pathway, through activation of phosphoinositide 3-kinase/Akt-G protein α_s-axin signaling axis (43) and inhibition of glycogen synthase kinase-3 (44). COX-2 is an important enzyme in PGE_2 generating pathway and its expression is highly inducible in various types of cells including macrophages (45). COX-2 protein was detected in infiltrating F4/80-positive cells (10) and CCR2-expressing cells. Moreover, CCL2 can induce COX-2 expression in human monocytes (46). Thus, CCL2 blocking may reduce the infiltration of COX-2-expressing F4/80-positive cells and depress COX-2 expression by infiltrating macrophages, and eventually inhibit the Wnt signaling pathway and neovascularization, resulting in retardation of cancer progression.

Based on our previous observation that blocking TNF-α reversed colon carcinoma

progression even after colon carcinoma was established, we proposed that drugs targeting TNF-α may be useful for the treatment of colon cancers, particularly those arising from chronic inflammation (10). Blocking CCL2 retarded colon cancer progression in this model with similar efficacy as TNF-α blockade, when given after multiple colon tumors were developed. Thus, drugs targeting CCL2 may be effective for the treatment of chronic inflammation-associated colon cancer, similarly to those targeting TNF-α. Because TNF-α has a wide variety of biological functions (9), TNF-α blocking agents can have serious adverse effects including the induction of bacterial, tuberculosis, and opportunistic infection (47). CCL2 has a limited biological function and therefore, drugs targeting CCL2 might have less severe adverse effects than those targeting TNF-α.

ACKNOWLEDGMENTS

We thank Dr. Joost J. Oppenheim (NCI-Frederick, Frederick, MD) for his critical reading of the manuscript and Dr. Naohisa Tomosugi (Kanazawa Medical University) for his technical advice on the use of an electrical pulse generator. We also thank Sanwa Chemical Co. for providing us with propagermanium.

AUTHOR CONTRIBUTIONS

B.K P. and F.I.K. performed most of experiments and wrote the manuscript. K.F. and T.W. contributed to the animal experiments using 7ND-expressing vector and immunohistochemical analysis. M.M.S. contributed to the animal experiments using propagermanium. T.K. contributed to histopathological analysis. K.E. constructed 7ND-expressing vector and contributed to the animal experiments using this vector. N.M. designed all of the studies, analyzed the data, and wrote the manuscript.

References

1. Fiocchi, C. Inflammatory bowel disease: Etiology and pathogenesis. Gastroenterology 1998; 115: 182-205.
2. Ullman, T, Croog, V, Harpaz, N, Sachar, D, Itzkowitz, S. Progression of flat low-grade dysplasia to advanced neoplasia in patients with ulcerative colitis. Gastroenterology 2003; 125: 1311-9.
3. Balkwill, F, Mantovani, A. Inflammation and cancer: back to Virchow? Lancet 2001; 357: 539-45.
4. Okayasu, I, Hatakeyama, S, Yamada, M, Ohkusa, T, Inagaki, Y, Nakaya, R. A novel method in the induction of reliable experimental acute and chronic ulcerative colitis in mice. Gastroenterology 1990; 98: 694-702.
5. Okayasu, I, Yamada, M, Mikami, T, Yoshida, T, Kanno, J, Ohkusa, T. Dysplasia and carcinoma development in a repeated dextran sulfate sodium-induced colitis model. J Gastroenterol Hepatol 2002; 17: 1078-83.
6. Okayasu, I, Ohkusa, T, Kajiura, K, Kanno, J, Sakamoto, S. Promotion of colorectal neoplasia in experimental murine ulcerative colitis. Gut 1996; 39: 87-92.
7. Greten, FR, Eckmann, L, Greten, TF, Park, JM, Li, ZW, Egan, LJ, et al. IKKβ links inflammation and tumorigenesis in a mouse model of colitis-associated cancer. Cell 2004 118: 285-96.
8. Reimund, JM, Wittersheim, C, Dumont, S, Muller, CD, Baumann, R, Poindron, P, et al. Mucosal inflammatory cytokine production by intestinal biopsies in patients with ulcerative colitis and Crohn's disease. J Clin Immunol 1996; 16: 144-50.
9. Wang, H, Czura, C J, Tracey, KJ. Tumor necrosis factor. In: Thomson, AW, Lotze, MT, editors. The Cytokine Handbook. 4th Edition. London: Elsevier Science Ltd.; 2003. p. 837-60.

10. Popivanova, BK, Kitamura, K, Wu, Y, Kondo, T, Kagaya, T, Kaneko, S, et al. Blocking TNF-α in mice reduces colorectal carcinogenesis associated with chronic colitis. J Clin Invest 2008; 118: 560-70.
11. Mazzucchelli, L, Hauser, C, Zgraggen, K, Wagner, HE, Hess, MW, Laissue, JA, et al. Differential *in situ* expression of the genes encoding the chemokines MCP-1 and RANTES in human inflammatory bowel disease. J Pathol 1996; 178: 201-6.
12. Reinecker, .C, Loh, EY, Ringler, DJ, Mehta, A, Rombeau, JL, MacDermott, RP. Monocyte-chemoattractant protein 1 gene expression in intestinal epithelial cells and inflammatory bowel disease mucosa. Gastroenterology 1995; 108: 40-50.
13. Uguccioni, M, Gionchetti, P, Robbiani, DF, Rizzello, F, Peruzzo, S, Campieri, M, et al. Increased expression of IP-10, IL-8, MCP-1 and MCP-3 in ulcerative colitis. Am J Pathol 1999; 155: 331- 6.
14. Matsushima, K, Larsen, CG, DuBois, GC, Oppenheim, JJ. Purification and characterization of a novel monocyte chemotactic and activating factor produced by a human myelomonocytic cell line. J Exp Med 1989; 169: 1485-90.
15. Zhang, Y, Rollins, BJ. A dominant negative inhibitor indicates that monocyte chemoattractant protein 1 functions as a dimer. Mol Cell Biol 1995; 15: 4851-5.
16. Yang, X, Lu, P, Ishida, Y, Kuziel, WA, Fujii, C, Mukaida, N. Attenuated liver tumor formation in the absence of CCR2 with a concomitant reduction in the accumulation of hepatic stellate cells, macrophages and neovascularization. Int J Cancer 2006; 118: 335-45.
17. Wong, LM, Myers, SJ, Tsou, CL, Gosling, J, Arai, H, Charo, IF. Organization and differential expression of the human monocyte chemoattractant protein 1 receptor gene. J Biol Chem 1997; 272: 1038-45.
18. Dwinell, MB, Eckmann, L, Leopard, JD, Varki, NM, Kagnoff, MF. Chemokine receptor expression by human intestinal epithelial cells. Gastroenterology 1999; 117: 359-67.

19. Charo, IF, Myers, SJ, Herman, A, Franci, C, Connolly, AJ, Coughlin, SR. Molecular cloning and functional expression of two monocyte chemoattractant protein 1 receptors reveals alternative splicing of the carboxyl-terminal tails. Proc Natl Acad Sci USA 1994; 91: 2752-6.
20. Wada, T, Yokoyama, H, Furuichi, K, Kobayashi, K, Harada, K, Naruto, M, et al. Intervention of crescentic glomerulonephritis by antibodies to monocyte chemotactic and activating factor (MCAF/MCP-1). FASEB J 1996; 10: 1418-25.
21. Kimura, H, Kasahara, Y, Kurosu, K, Sugito, K, Takiguchi, Y, Terai, M, et al. Alleviation of monocrotaline-induced pulmonary hypertension by antibodies to monocyte chemotactic and activating factor/monocyte chemoattractant protein-1. Lab Invest 1998; 78: 571-8.
22. Moore, BB, Paine III, R, Christensen, PJ, Moore, TA, Sitterding, S, Ngan, R, et al. Protection from pulmonary fibrosis in the absence of CCR2 signaling. J Immunol 2001; 167: 4368-77.
23. Boring, L, Gosling, J, Cleary, M, Charo, IF. Decreased lesion formation in $CCR2^{-/-}$ mice reveals a role for chemokines in the initiation of atherosclerosis. Nature 1998; 394: 894-7.
24. Izikson, L, Klein, RS, Charo, IF, Weiner, HL, Luster, AD. Resistance to experimental autoimmune encephalomyelitis in mice lacking the CC chemokine receptor (CCR) 2. J Exp Med 2000; 192: 1075-80.
25. Shahrara S, Proudfoot, AEI, Park, CC, Volin, MV, Haines, GK, Woods, JM, et al. Inhibition of monocyte chemoattractant protein-1 ameliorates rat adjuvant-induced arthritis. J Immunol 2008; 180: 3447-56.
26. Guijarro, LG, Mate, J, Gisbert, JP, Perez-Calle, JL, Marin-Jimenez, I, Arriaza, E, et al. N-acetyl-L-cysteine combined with mesalamine in the treatment of ulcerative colitis: Randomized, placebo-controlled pilot study. World J Gasrtoenterol 2008; 14: 2851-7.

27. Andreas, PG, Beck, PL, Mizoguchi, E, Mizoguchi, A, Bhan, AK, Dawson, T, et al. Mice with a selective deletion of the CC chemokine receptors 5 or 2 are protected from dextran sodium sulfate-mediated colitis: lack of CC chemokine receptor 5 expression results in a $NK1.1^+$ lymphocyte-associated Th2-type immune response in the intestine. J Immunol 2000; 164: 6303-12.

28. Salcedo, R, Ponce, ML, Young, HA, Wasserman, K, Ward, JM, Kleinman, HK, et al. Human endothelial cells express CCR2 and respond to MCP-1: direct role of MCP-1 in angiogenesis and tumor progression. Blood 2000; 96: 34-40.

29. Carulli, MT, Ong, VH, Ponticos, M, Shiwen, X, Abraham, DJ, Black, CM, et al. Chemokine receptor CCR2 expression by systemic sclerosis fibroblasts: evidence for autocrine regulation of myofibroblast differentiation. Arthritis Rheum 2005; 52: 3772-82.

30. Klopp, AH, Spaeth, EL, Dembinski, JL, Woodward, WA, Munshi, A, Meyn, RE, et al. Tumor irradiation increases the recruitment of circulating mesenchymal stem cells into the tumor microenvironment. Cancer Res 2007; 67: 11687-95.

31. Lu, Y, Cai, Z, Galson, DL, Xiao, G, Liu, Y, George, DE, et al. Monocyte chemotactic protein-1 (MCP-1) acts as a paracrine and autocrine factor for prostate cancer growth and invasion. Prostate 2006; 66: 1311-8.

32. Spring, H, Schuler, T, Arnold, B, Hammerling, G, Ganss, R. Chemokines direct endothelial progenitors into tumor neovessels. Proc Natl Acad Sci USA 2005; 102: 18111-6.

33. Moore, BB, Kolodsick, JE, Thannickal, VJ, Cooke, K, Moore, TA, Hogaboam, C, et al. CCR2-mediated recruitment of fibrocytes to the alveolar space after fibrotic injury. Am J Pathol 2005; 166: 675-84.

34. Tokuyama, H, Ueha, S, Kurachi, M, Matsushima, K, Moriyasu, F, Blumberg, RS, et al. The simultaneous blockade of chemokine receptors CCR2, CCR5 and CXCR3 by a

non-peptide chemokine receptor antagonist protects mice from dextran sodium sulfate-mediated colitis. Int Immunol 2005; 17: 1023-34.

35. Sica, A, Allavena, P, Mantovani, A. Cancer related inflammation: The macrophage connection. Cancer Lett 2008; 264: 204-15.
36. Graves, DT, Jiang, YL, Williamson, MJ, Valente, AJ. Identification of monocyte chemotactic activity produced by malignant cells. Science 1989; 245: 1490-3.
37. Loberg, RD, Ying, C, Craig, M, Day, LL, Sargent, E, Neeley, C, et al. Targeting CCL2 with systemic delivery of neutralizing antibodies induces prostate cancer regression in vivo. Cancer Res 2007; 67: 9417-24.
38. Gong, JH, Clark-Lewis, I. Antagonists of monocyte chemoattractant protein 1 identified by modification of functionally critical NH_2-terminal residues. J Exp Med 1995; 181: 631-40.
39. Kitamoto, S, Egashira K. Anti-monocyte chemoattractant protein-1 gene therapy for cardiovascular diseases. Expert Rev Cardiovasc Ther 2003; 1: 393-400.
40. Furuichi, K, Wada, T, Iwata, Y, Kitagawa, K, Kobayashi, K, Hashimoto, H, et al. Gene therapy expressing amino-terminal truncated monocyte chemoattractant protein-1 prevents renal ischemia-reperfusion injury. J Am Soc Nephrol 2003; 14: 1066-71.
41. Yokochi, S, Hashimoto, H, Ishiwata, Y, Shimokawa, H, Haino, M, Terashima, Y, et al. An anti-inflammatory drug, propagermanium, may target GPI-anchored proteins associated with an MCP-1 receptor, CCR2. J Interferon Cytokine Res 2001; 21: 389-98.
42. Iniguez, MA, Rodriguez, A, Volpert, OV, Fresno, M, Redondo, JM. Cyclooxygenase-2: a therapeutic target in angiogenesis. Trends Mol Med 2003; 9:73-8.
43. Castellone, MD, Teramoto, H, Williams, BO, Druey, KM, Gutkind, JS. Prostaglandin E_2 promotes colon cancer cell growth through a G_s-axin-β-catenin signaling aixs. Science 2005; 310:1504-10.

44. Shao, J, Jung, C, Liu, C, Sheng, H. Prostaglandin E_2 stimulates the β-catenin/T cell factor-dependent transcription in colon cancer. J Biol Chem 2005; 280: 26565-72.

45. Arias-Negrete S, Keller, K, Chadee, K. Proinflammatory cytokines regulate cyclooxygenase-2 mRNA expression in human macrophages. Biochem Biophys Res Commun 1995; 208: 582-9.

46. Tanaka, S, Tatsuguchi, A, Futagami, S, Gudis, K, Wada, K, Seo, T, et al. Monocyte chemoattractant protein 1 and macrophage cyclooxygenase 2 expression in colonic adenoma. Gut 2006; 55: 54-61.

47. Rutgeerts, P, Sandborn, WJ, Feagan, BG, Reinisch, W, Olson A, Johanns, J, et al. Infliximab for induction and maintenance therapy for ulcerative colitis. N Engl J Med 2005; 353: 2462-76.

Figure Legends

Figure 1. Tumor formation in WT and CCR2-deficient (CCR2KO) mice after AOM and DSS treatment. (**A**) Tumor numbers. Colons were removed at day 56 to determine the numbers of macroscopic tumors. Results are presented as mean ± SD (n=10 animals). **, $p<0.01$ versus WT mice. (**B**) CCL2 gene expression in the colons of WT mice. The levels of CCL2 mRNA were quantified by real-time RT-PCR as described in Materials and Methods, and normalized to the level of GAPDH mRNA. *, $p<0.05$, **, $p<0.01$ versus untreated (control) mice. (**C, D**) Immunohistochemical detection of CCL2-positive (**C**) and CCR2-positive cells (**D**) in the colons. Colons were obtained from WT mice at the indicated time points. Immunohistochemical analysis was conducted as described in Materials and Methods. Representative results from 5 independent animals are shown here. Scale bars, 50 μm.

Figure 2. Microscopical analysis of colon tissues.

(**A**) Colons were removed at the indicated time intervals, fixed and stained with hematoxylin and eosin. Representative results from 5 mice are shown here. (**B**) Immunohistochemical staining for β-catenin. Colons were removed at the indicated time intervals from WT and CCR2-deficient mice and immunostained with anti-β-catenin antibody as described in Materials and Methods. Representative results from 5 mice are shown here. (**C**) The numbers of F4/80-positive cells were counted as described in Materials and Methods and are shown here. All values represent the mean ± SD (n=10 animals), *, $p<0.05$, **, $p<0.01$ vs. untreated (control) mice. Scale bars, 50 μm (**A**), 20 μm (**B**).

Figure 3. Colon tumor formation in bone marrow chimeric mice.

Bone marrow chimeric mice were generated and subjected to AOM and DSS treatment as described in Materials and Methods. Colons were removed at day 56 and the tumor numbers

were determined macroscopically. The bars represent the mean of each group; each symbol represents the tumor numbers of each animal (n = 4 to 5), *, $p<0.05$, **, $p<0.01$; NS, not significant.

Figure 4. COX-2 expression in the colons.

(**A**) Quantitative RT-PCR was performed on total RNAs extracted from the colons at the indicated time points as described in Materials and Methods. The levels of COX-2 mRNA were normalized to the levels of GAPDH mRNA. *, $p<0.05$, **, $p<0.01$, vs. untreated mice. (**B, C**) Immunohistochemical detection of COX-2 expressing cells. Colons were obtained from WT mice at the indicated time points and immunostained with anti-COX-2 antibody as described in Materials and Methods. Representative results from 6 independent animals are shown in **B.** The numbers of COX-2 expressing cells were determined. Mean±SD were calculated and are shown in **C.** *, $p<0.05$, **, $p<0.01$, vs. untreated mice. (**D**) A double-color immunofluorescence analysis on COX-2 expression by CCR2-expressing cells. Colons were obtained from WT mice and immunolabeled with anti-CCR2 (left panel) and anti-COX-2 antibodies (middle panel). Fluorescence was digitally merged in the right panel. Representative results from 6 independent experiments are shown here. Scale bars, 20 μm (**B, D**).

Figure 5. The effects of 7ND-expressing vector injection on colon carcinogenesis. (**A**) Macroscopic evaluation of the tumors. Colons were removed on day 67 from WT mice, injected with 7ND-expressing or with pcDNA3 vector. Representative results from 7 to 8 independent animals are shown here. (**B**) The tumor numbers and sizes were determined macroscopically. The bars represent the mean of each group. Each symbol represents the tumor numbers of each animal or the average size of the tumors of each animal. **, $p<0.01$ vs. WT mice injected with pcDNA3 vector. (**C**) Colons were processed to hematoxylin and eosin

staining and representative results from 6 independent animals are shown here. Scale bar, 50 μm. (**D**) F4/80-positive macrophages were enumerated as described in Materials and Methods. All values represent the mean ± SD (n=5 animals). *, $p<0.05$, **, $p<0.01$, vs. WT mice injected with pcDNA3 vector.

Figure 6. The effect of 7ND-expressing vector injection on colon carcinoma progression. (**A**) COX-2 expression after 7ND-expressing vector injection. Quantitative RT-PCR analysis for COX-2 mRNA (left panel) and immunohistochemical analysis with anti-COX-2 antibody (right panel) were at the indicated time points as described in Materials and Methods. The levels of COX-2 mRNA were normalized to the levels of GAPDH mRNA (left panel), while the numbers of COX-2-expressing cells were determined on 5 independent animals as described in Materials and Methods (right panel). The mean ± SD were calculated on all values and are shown here. *, $p<0.05$ vs. WT mice injected with pcDNA3 vector; **, $p<0.01$, vs. WT mice injected with pcDNA3 vector. (**B**) The vascular areas were determined as described in Materials and Methods and are shown in here. *, $p<0.05$ vs. WT mice injected with pcDNA3 vector. (**C**) The β-catenin nuclear localization ratio was determined as the ratio of the numbers of tumor nuclei with β-catenin localization to the total number of tumor nuclei per field. At least 5 randomly chosen fields at x 400 magnification were examined. All values represent the mean ± SD, *, $p<0.05$, vs. WT mice injected with pcDNA3 vector. (**D**) The numbers of cytokeratin 20-positive cells were determined on 5 randomly chosen visual fields at x 400 magnification. All values represent the mean ± SD, **, $p<0.01$, vs. WT mice injected with pcDNA3 vector.

Figure 1

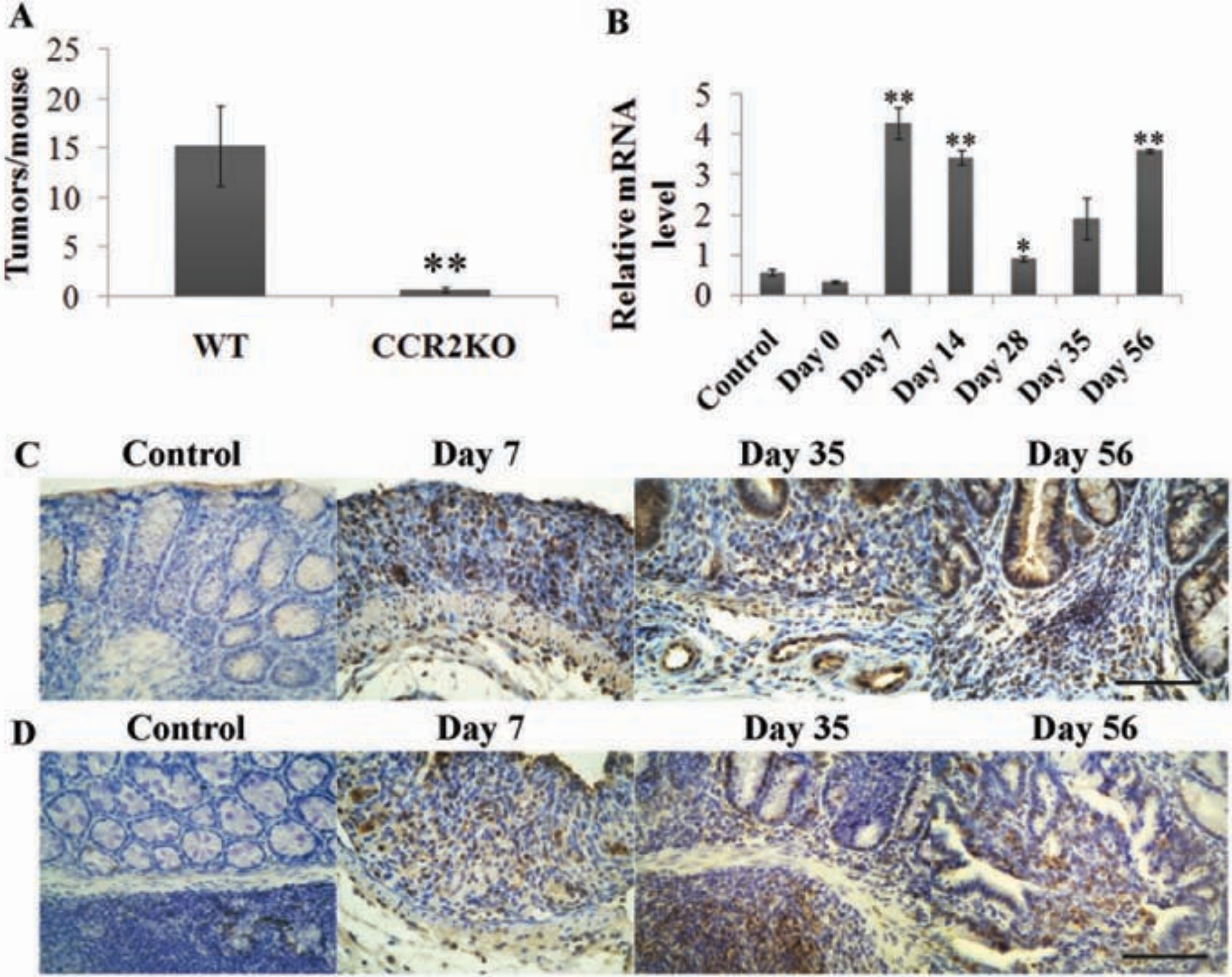
A
Tumors/mouse
25
20
15
10
5
0
**
WT
CCR2KO
B
Relative mRNA level
5
4
3
2
1
0
**
**
*
**
Control
Day 0
Day 7
Day 14
Day 28
Day 35
Day 56
C
Control
Day 7
Day 35
Day 56
D
Control
Day 7
Day 35
Day 56

Figure 2

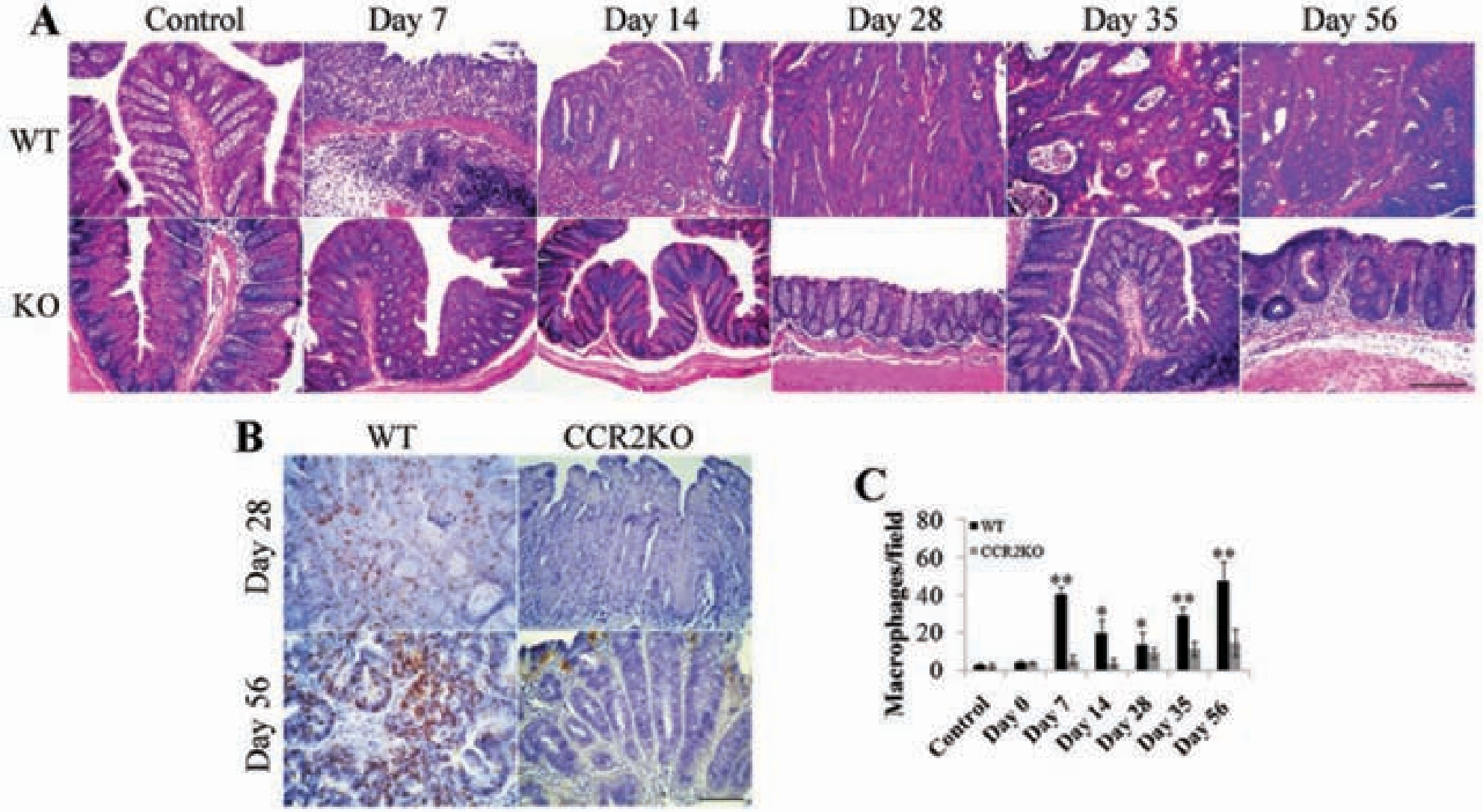
A
Control
Day 7
Day 14
Day 28
Day 35
Day 56
WT
KO
B
WT
CCR2KO
Day 28
Day 56
C
Macrophages/field
80
60
40
20
0
WT
CCR2KO
Control
Day 0
Day 7
Day 14
Day 28
Day 35
Day 56

Figure 3

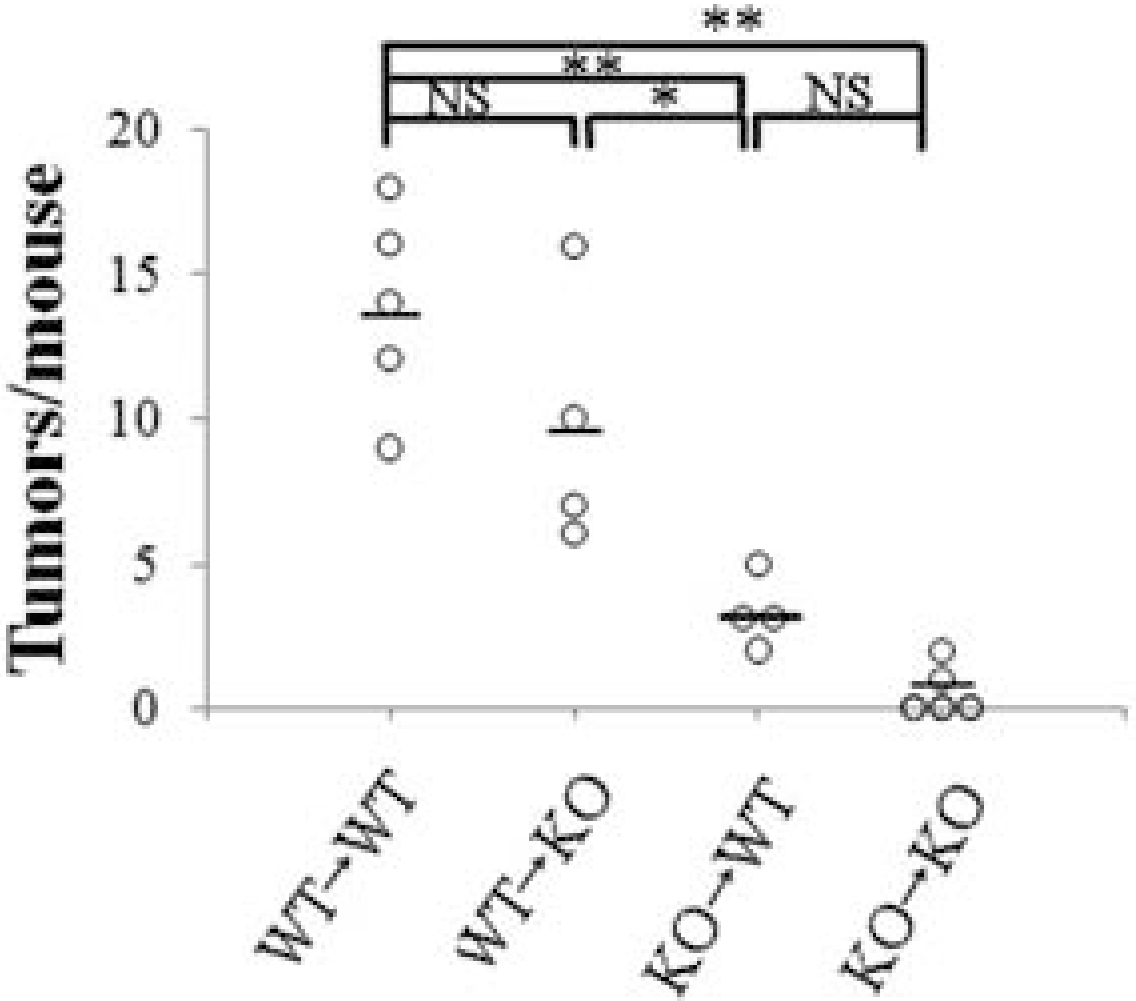

Figure 4

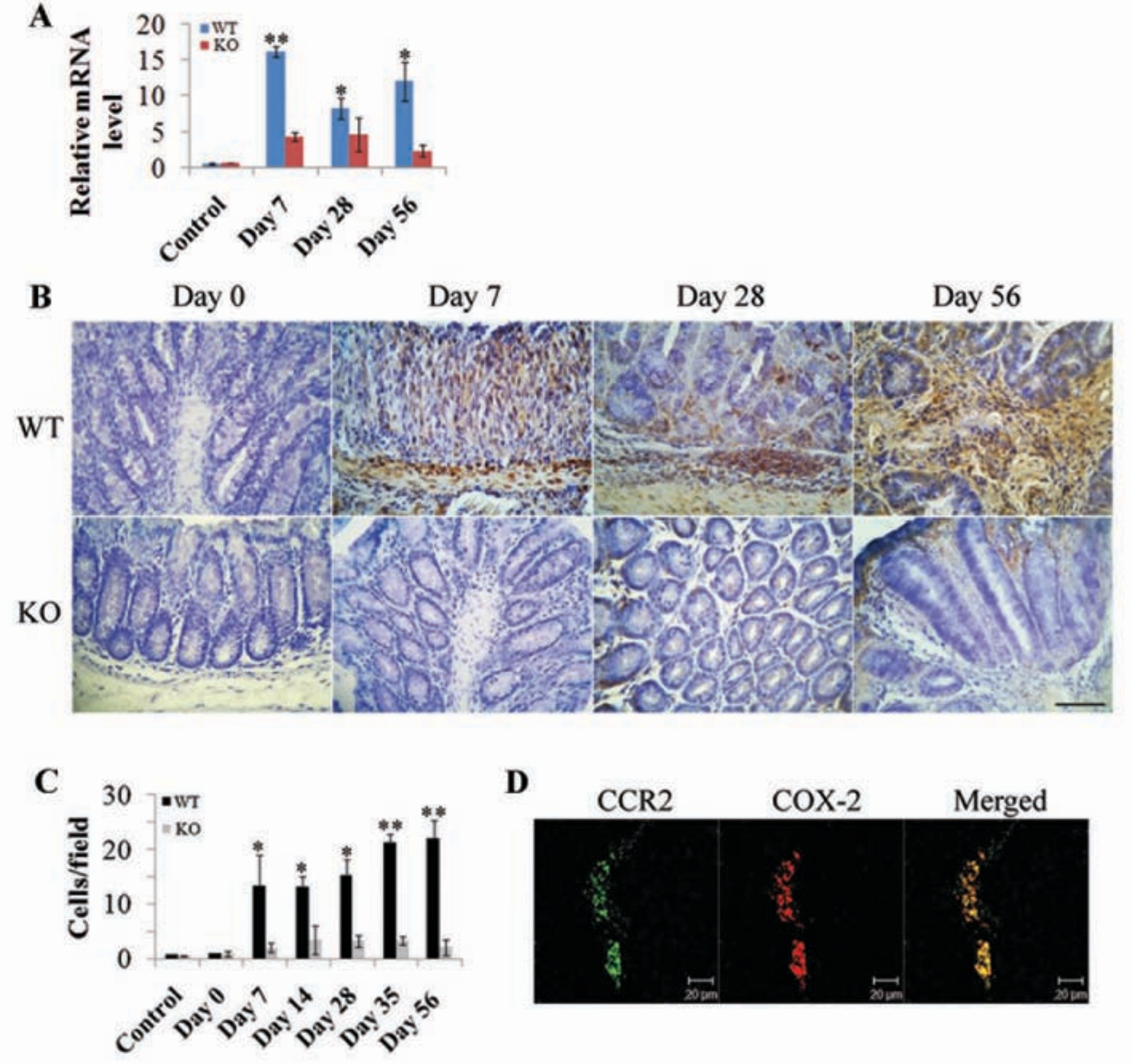
A
Relative mRNA level
20
15
10
5
0
WT
KO
**
*
*
Control
Day 7
Day 28
Day 56
B
Day 0
Day 7
Day 28
Day 56
WT
KO
C
Cells/field
30
20
10
0
WT
KO
*
*
*
**
**
Control
Day 0
Day 7
Day 14
Day 28
Day 35
Day 56
D
CCR2
COX-2
Merged
20 μm
20 μm
20 μm

Figure 5

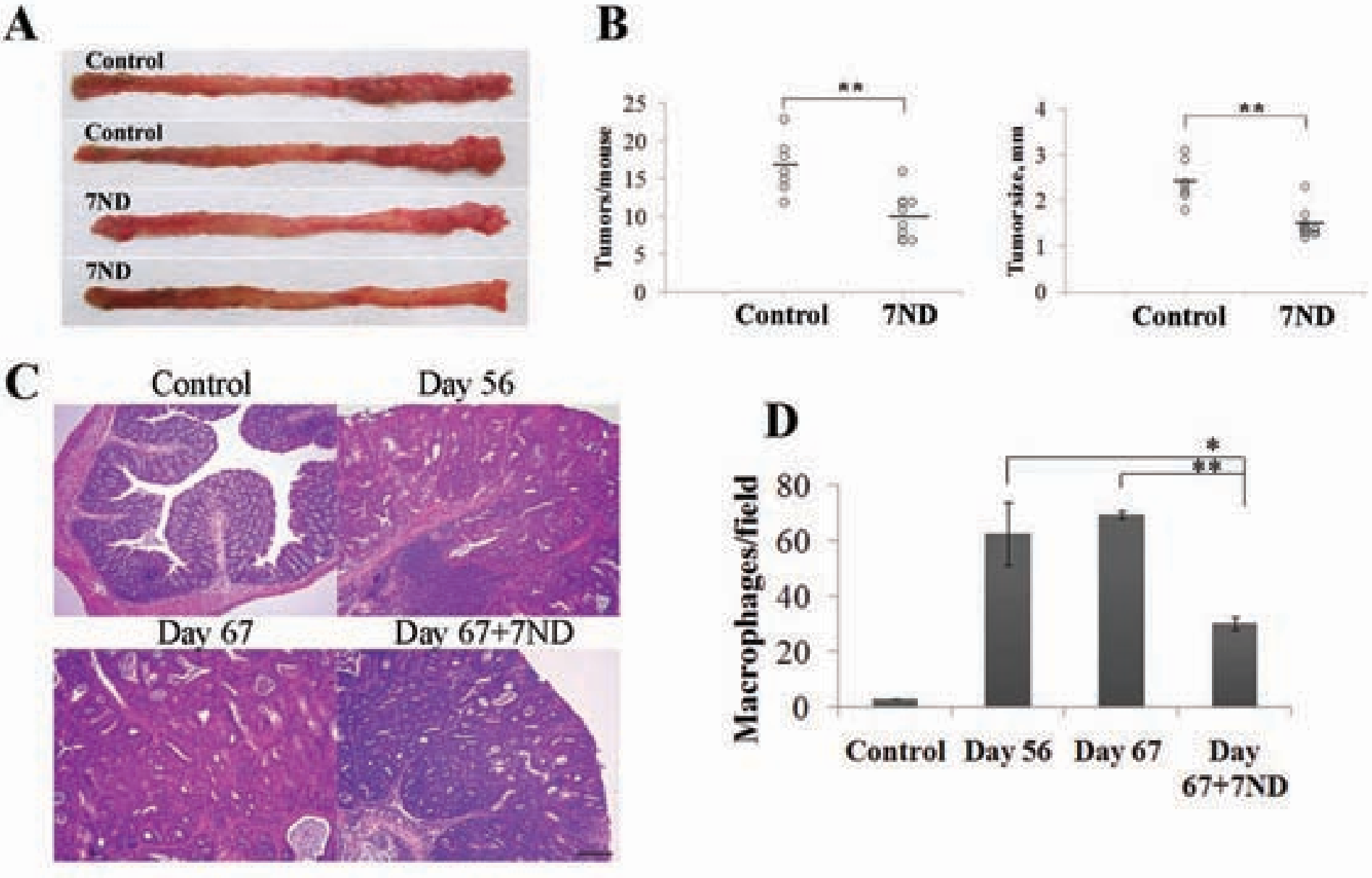
A
Control
Control
7ND
7ND
B
Tumors/mouse
25
20
15
10
5
0
**
Control
7ND
Tumor size, mm
4
3
2
1
0
**
Control
7ND
C
Control
Day 56
Day 67
Day 67+7ND
D
Macrophages/field
80
60
40
20
0
*
**
Control
Day 56
Day 67
Day 67+7ND

Figure 6

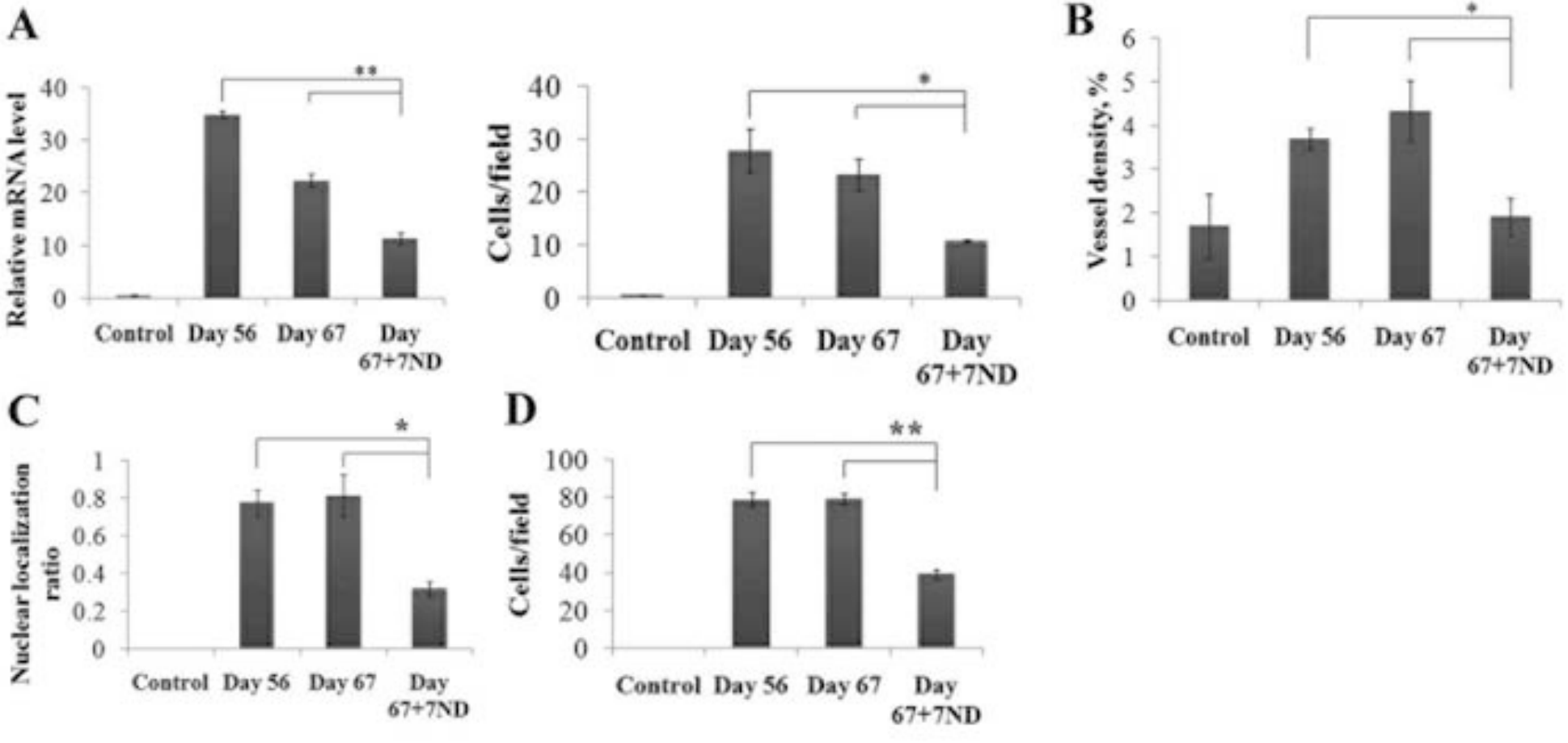
A
Relative mRNA level
40
30
20
10
0
**
Control
Day 56
Day 67
Day 67+7ND
Cells/field
40
30
20
10
0
*
Control
Day 56
Day 67
Day 67+7ND
B
Vessel density, %
6
5
4
3
2
1
0
*
Control
Day 56
Day 67
Day 67+7ND
C
Nuclear localization ratio
1
0.8
0.6
0.4
0.2
0
*
Control
Day 56
Day 67
Day 67+7ND
D
Cells/field
100
80
60
40
20
0
**
Control
Day 56
Day 67
Day 67+7ND